Polyhedron 189 (2020) 114723

Contents lists available at ScienceDirect

Polyhedron

journal homepage: www.elsevier.com/locate/poly

Analysis of supramolecular interactions directing crystal packing of novel mononuclear chloranilate-based complexes: Different types of hydrogen bonding and π-stacking

Lidija Kanižaj [a], Vedran Vuković [b], Emmanuel Wenger [b], Marijana Jurić [a,*], Krešimir Molčanov [a,*]

[a] Ruđer Bošković Institute, Bijenička cesta 54, 10000 Zagreb, Croatia
[b] CRM² CNRS, UMR 7036, Institut Jean Barriol, Université de Lorraine, BP 70239 Vandoeuvre-lès-Nancy, France

ARTICLE INFO

Article history:
Received 17 April 2020
Accepted 24 July 2020
Available online 30 July 2020

Keywords:
Chloranilate ligand
Crystal structure
Crystal engineering
Hydrogen-bonding
π-interaction
Hirshfeld surfaces

ABSTRACT

Three novel mononuclear chloranilate complexes, $\{[Cu(bpy)(H_2O)(C_6O_4Cl_2)]\cdot H_2O\}_6$ (**2**; bpy = 2,2′-bipyridine), $[Cu(bpy)(C_6O_4Cl_2)]\cdot 0{\cdot}5H_2O$ (**3**) and $[(n\text{-}Bu)_4N][Fe(H_2O)_2(C_6O_4Cl_2)_2]\cdot 2H_2O$ (**4**) have been prepared using building blocks $[M^{III}(C_6O_4Cl_2)_3]^{3-}$ (M^{III} = Fe and Cr), which proved to be a source of the chloranilate groups. Namely, by applying layering technique an unexpected partial decomposition of used metalate anions leads to the release of the chloranilate ligand from the coordination sphere of chromium(III) and iron(III) ions. During crystallization process, the released group is consequently coordinated to copper(II) ion in the reaction mixtures, yielding crystals of **2** or **3**. Crystals of compound **4** have been formed as a result of the ligand exchange process. Also, it appears that slow diffusion and the solvent mixture used herein causes formation of the crystals of the quality needed for X-ray analysis of the starting building block $[(n\text{-}Bu)_4N]_3[Cr(C_6O_4Cl_2)_3]$ (**1**), whose crystal structure has not been known. Interestingly, compound $\{[Cu(bpy)(C_6O_4Cl_2)(H_2O)]\cdot H_2O\}_6$ (**2**) displays an unusual case of hypersymmetry with $Z' = 6$. Analysis of crystal structures and intermolecular interactions of **1**–**4** revealed role of hydrogen bonding and π-interactions in stabilization of crystal lattices, further characterized by fingerprint plots derived from the Hirshfeld surfaces (HS). Two phases of compound **4** were identified: at low-temperature (100 K) **4-LT** and at room-temperature **4-RT**, with similar unit-cell parameters. However, different positions and orientations of water molecules result in completely different hydrogen-bonding patterns.

1. Introduction

One of the most attractive topics in chemical science is design and preparation of molecular materials based on targeted physical properties such as long-rage magnetic order, spin crossover, electrical conductivity, superconductivity, porosity, etc., especially those multifunctional in which two (or more) functional properties are strongly coupled providing its response to the external stimulus [1,2].

The oxalate group has been demonstrated to be one of the most versatile ligands used in the preparation of these materials. Due to its various possibilities of coordination to the metal centres as well as its ability to mediate magnetic interactions between paramagnetic metal ions, a large number of oxalate-based transition-metal species of different nuclearity and dimensionality have been synthesized and characterized, many of them having tunable magnetic frameworks [3]. Most of the oxalate-based molecular magnets described to date have been obtained by the "complex-as-ligand approach". In this synthetic strategy, a molecular building block, the tris(oxalato)metalate $[M^{III}(C_2O_4)_3]^{3-}$ anion (M^{III} = Cr, Fe, Ru, Rh, Mn or V) is used as a ligand towards other metal cations in the preparation mostly of two- (2D) and three-dimensional (3D) extended systems of the general formula $[M_a^{II/III}Mb_b^{I/II}(C_2O_4)_3]_n^{2n-/n-}$ [4].

Inspired by the interesting properties of the investigated oxalate-based systems, more recent studies involved a class of sterically larger ligands, topologically analogous to the oxalate dianion: 2,5-dihydroxy-1,4-benzoquinone (H_2dhbq) and its derivatives, which are obtained by substituting the hydrogens at the positions 3 and 6 of the $dhbq^{2-}$ by halogen atoms or functional groups. Thus formed moiety is known as the anilate ($C_6O_4X_2^{2-}$ = X_2An^{2-}). Anilic and its anions have uniquely electronic structure which changes upon (de)protonation and coordination to metal cations. This is achieved by re-arrangement of π electrons: in

* Corresponding authors.
E-mail addresses: Marijana.Juric@irb.hr (M. Jurić), Kresimir.Molcanov@irb.hr (K. Molčanov).

https://doi.org/10.1016/j.poly.2020.114723
0277-5387/

neutral species they are localized so the anilate ring has a *p*-quinoid structure, while in mono- and dianions π electrons are delocalized in the fragment O—C—C(–X)–C—O [5] and these fragments are separated by single C—C bonds. Coordinated species behave differently: anilate acting as bridging (bis)bidentate ligands have structure similar to dianions, while those acting as terminal bidentate ligands have an *o*-quinoid structure with localized π electrons [5]. A result of this structural variability is propensity for π-stacking which is usually stronger than in aromatic systems [6–8]. In fact, planar chloranilate complexes stack with relatively short interplanar separations (<3.3 Å) and anilate mono anions form the strongest observed stacking interactions of closed-shell rings [6–8].

In general, anilates are very interesting building blocks due to: (*i*) a variety of coordination modes to metal centres; (*ii*) their ability to mediate electronic effects between paramagnetic metal ions; (*iii*) they are easy to modify or functionalize in order to tune the exchange coupling through them by simply changing the X group (X = H, F, Cl, Br, I, NO_2, OH, CN, Me, Et, etc.), while their modification does not influence their coordination mode; (*iv*) the capability of an easy reduction into the radical anionic form; (*v*) presence of different substituents in the anilato moiety give rise to intermolecular interactions such as hydrogen-bonding, halogen-bonding, π-stacking and dipolar interactions which may have an effect on the physical properties of the resulting material; (*vi*) they are sterically larger than the oxalate group and produce structures with much larger voids where many different cations and solvent molecules can be included forming multifunctional molecular materials [6–14].

The most intensively studied anilate ligand is chloranilate (X = Cl), which has been used as the appropriate ligand, alone or in combination with other ligands (mostly *N*-donors), to prepare coordination compounds with different dimensionalities and structures, as monomers, dimers and oligomers to extended 1D, 2D, and 3D structures [6,13]. The 2D and 3D homo- and heterometallic lattices, also obtained in the oxalate family, have been prepared using tris(anilato)metalate building blocks $[M^{III}(C_6O_4X_2)_3]^{3-}$ (M^{III} = Fe and Cr; X = Cl and Br). A new family of heterometallic 2D honeycomb lattices containing chirality and porosity or long-range magnetic order were studied [11].

In our previous works we reported structural and magnetic properties of heterometallic oxalate-bridged coordination polymers of different dimensionality obtained using $[M^{III}(C_2O_4)_3]^{3-}$ (M^{III} = Cr, Mn and Fe) as building blocks in reaction with other metal centres [15–18]. Motivated by interesting results we have expanded our research to the preparation of novel compounds using $[M^{III}(C_6O_4Cl_2)_3]^{3-}$ (M^{III} = Cr and Fe) as ligands toward copper(II) ions, with the addition of the *N*-donor ligands [12,19–21]. It is known that the use of the capping ligands, together with the stabilization of the solid-state structures, can control and influence the dimensionality of coordination systems [4].

Three novel mononuclear chloranilate complexes {[Cu(bpy)$(H_2O)(C_6O_4Cl_2)]\cdot H_2O\}_6$ (**2**; bpy = 2,2′-bipyridine), [Cu(bpy)$(C_6O_4Cl_2)]\cdot 0{\cdot}5H_2O$ (**3**) and $[(n\text{-}Bu)_4N][Fe(H_2O)_2(C_6O_4Cl_2)_2]\cdot 2H_2O$ (**4**) have been prepared using approach "building-block chemistry" in the form of single-crystals, also as previously familiar compound $[(n\text{-}Bu)_4N]_3[Cr(C_6O_4Cl_2)_3]$ (**1**) known in the form of powder [10]. Detailed analysis of their crystal structures and intermolecular interactions has been done. The search of the Cambridge Structural Database (CSD) found only four mononuclear copper(II) complexes containing 2,2′-bipyridine as *N*-ligand [3]: two square-planar polymorphs of anhydrous [Cu(bpy)$(C_6O_4Cl_2)$], then [Cu(bpy)$(C_6O_4Cl_2)(H_2O)]\cdot CH_3OH$ with square-pyramidal coordination of copper(II) atom, and $[Cu(bpy)_2(C_6O_4Cl_2)]\cdot 0.5bpy\cdot H_2O$ or $[Cu(bpy)_2(C_6O_4Cl_2)]\cdot 0.5bpy\cdot 2H_2O$ with octahedral coordination modes [19].

2. Experimental

2.1. Materials and physical measurements

All chemicals were purchased from commercial sources and used without further purification. The starting species $[(n\text{-}Bu)_4N]_3[M^{III}(C_6O_4Cl_2)_3]$ (M^{III} = Cr, Fe) were prepared according to the method described in the literature [10,22]. Elemental analyses for C, H and N were performed with a Perkin–Elmer Model 2400 microanalytical analyser. The infrared spectra were recorded in the 4000–350 cm^{-1} region with samples as KBr pellets, with a Bruker Alpha-T spectrometer.

2.2. Synthesis

2.2.1. Preparation of $[(n\text{-}Bu)_4N]_3[Cr(C_6O_4Cl_2)_3]$ (**1**) and $\{[Cu(bpy)(H_2O)(C_6O_4Cl_2)]\cdot H_2O\}_6$ (**2**)

An aqueous solution (4 mL) containing $CuCl_2\cdot 2H_2O$ (0.009 g; 0.05 mmol) and 2,2′-bipyridine (0.008 g; 0.05 mmol) was layered with an acetonitrile solution (6 mL) of $[(n\text{-}Bu)_4N]_3[Cr(C_6O_4Cl_2)_3]$ (0.068 g; 0.05 mmol) in a test tube. Dark red plate-like crystals of chromium precursor **1** were formed after two weeks in the open test tube together with few dark red crystals of compound **2**. Also dark red powder having coordinated bipyridine and chloranilate ligands (confirmed by IR spectroscopy) was observed after the evaporation process was completed. Crystals were washed with a small amount of water and dried in air. Two kinds of single-crystals were separated mechanically. Yield: 20% (**1**). Anal. Calc. for $C_{66}H_{108}Cl_6CrN_3O_{12}$ (**1**; *Mr* = 1400.25): C, 56.61; H, 7.77; N, 3.00. Found: C, 56.60; H, 7.79; N, 3.02%. IR data (KBr, cm^{-1}): 3432 (m), 2960 (m), 2921 (m), 2875 (w), 1658 (sh), 1644 (m), 1630 (m), 1612 (sh), 1532 (vs), 1468 (m), 1383 (m), 1353 (s), 1303 (m), 1250 (w), 1162 (w), 1108 (w), 1060 (w), 1028 (w), 1001 (w), 878 (w), 841 (m), 668 (w), 611 (m), 599 (sh), 573 (w), 508 (w), 466 (w). Anal. Calc. for $C_{16}H_{12}Cl_2CuN_2O_6$ (**2**; *Mr* = 462.72): C, 41.53; H, 2.61; N, 6.05. Found: C, 41.50; H, 2.62; N, 6.05%. IR data (KBr, cm^{-1}): 3450 (w), 1709 (s), 1650 (m), 1608 (m), 1542 (vs), 1519 (w), 1493 (sh), 1485 (s), 1450 (m), 1352 (s), 1321 (m), 1301 (m), 1270 (sh), 1252 (w), 1172 (w), 1159 (w), 1110 (w), 1038 (w), 998 (w), 847 (m), 773 (w), 730 (w), 605 (m), 576 (m), 508 (w).

2.2.2. Preparation of $[Cu(bpy)(C_6O_4Cl_2)]\cdot 0{\cdot}5H_2O$ (**3**)

An acetonitrile solution (6 mL) of $[(n\text{-}Bu)_4N]_3[Fe(C_6O_4Cl_2)_3]$ (0.070 g; 0.05 mmol) was carefully laid above an aqueous solution (4 mL) containing $CuCl_2\cdot 2H_2O$ (0.009 g; 0.05 mmol) and 2,2′-bipyridine (0.008 g; 0.05 mmol) into a test tube. The X-ray quality dark red polyhedra of **3** were formed after two weeks in the open tube, washed with a small amount of water and dried in air. After evaporation black powder consisting coordinated chloranilate groups (confirmed by IR spectroscopy) was observed at the bottom of the tube. Yield: 32%. Anal. Calc. for $C_{16}H_{8.15}Cl_2CuN_2O_{4.13}$ (**3**; *Mr* = 429.00): C, 44.79; H, 1.91; N, 6.53. Found: C, 44.81; H, 1.88; N, 6.54%. IR data (KBr, cm^{-1}): 3445 (w), 1710 (s), 1648 (m), 1611 (m), 1539 (vs), 1518 (w), 1496 (sh), 1480 (s), 1450 (m), 1350 (s), 1320 (m), 1301 (m), 1268 (sh), 1251 (w), 1172 (w), 1158 (w), 1107 (w), 1035 (w), 999 (w), 846 (m), 775 (w), 730 (w), 604 (m), 576 (m), 509 (w).

2.2.3. Preparation of $[(n\text{-}Bu)_4N][Fe(H_2O)_2(C_6O_4Cl_2)_2]\cdot 2H_2O$ (**4**)

An aqueous solution (4 mL) of $CuCl_2\cdot 2H_2O$ (0.009 g; 0.05 mmol) and 1,10-phenanthroline (0.010 g; 0.05 mmol) was layered with an acetonitrile solution (6 mL) of $[(n\text{-}Bu)_4N]_3[Fe(C_6O_4Cl_2)_3]$ (0.071 g; 0.05 mmol) in an open test tube. After two months brown rod-like single crystals of compound **4** were obtained, washed with a small amount of water and dried in air. Black powder containing coordinated phenantroline and chloranilate groups (confirmed by IR spectroscopy) was formed after evaporation of the solvent from

the reaction mixture. Yield: 19%. Anal. Calc. for $C_{28}H_{44}Cl_4FeNO_{12}$ (**4**; *Mr* = 784.29): C, 42.88; H, 5.65; N, 1.79. Found: C, 42.87; H, 5.63; N, 1.82%. IR data (KBr, cm^{-1}): 3450 (m), 2961 (m), 2924 (m), 2875 (w), 1647 (s), 1631 (sh), 1571 (sh), 1538 (vs), 1527 (sh), 1514 (sh), 1483 (s), 1459 (sh), 1370 (sh), 1350 (vs), 1321 (s), 1298 (sh), 1251 (m), 1149 (w), 1062 (w), 1024 (w), 1000 (m), 885 (w), 848 (s), 796 (w), 736 (w), 603 (m), 576 (m), 512 (m).

2.3. Single-crystal X-ray structural study

Single crystal of compound **3** was measured on an Oxford Diffraction Xcalibur Nova R diffractometer (microfocus Cu tube) equipped with an Oxford Instruments CryoJet liquid nitrogen cooling device. Program package CrysAlis PRO [23] was used for data reduction and multi-scan absorption correction. Single crystals of

Table 1
Crystallographic data and details of data collection and refinements for compounds **1**–**4**.

Compound	**1**	**2**	**3**
Empirical formula	$C_{66}H_{108}Cl_6CrN_3O_{12}$	$C_{16}H_{12}Cl_2CuN_2O_6$	$C_{16}H_{8.15}Cl_2CuN_2O_{4.13}$
Formula wt./g mol^{-1}	1400.25	462.72	429.00
Colour	dark red	dark red	dark red
Crystal dimensions/mm	0.23 × 0.14 × 0.09	0.16 × 0.14 × 0.10	0.25 × 0.20 × 0.12
Space group	$P\bar{1}$	$P2_1/c$	$C2/c$
a / Å	12.120(5)	26.918(2)	24.9698(3)
b / Å	15.526(5)	9.6585(9)	7.44910(10)
c / Å	21.105(5)	39.554(4)	16.8646(2)
α / °	92.667(5)	90	90
β / °	103.786(5)	100.816(3)	103.7940(10)
γ / °	103.069(5)	90	90
Z	2	24	8
V / $Å^3$	3736(2)	10100.9(16)	3046.39(7)
D_{calc} / g cm^{-3}	1.245	1.826	1.871
λ / Å	0.71073 (Mo*K*α)	0.71073 (Mo*K*α)	1.54179 (CuKα)
μ/ mm^{-1}	0.424	1.654	5.513
Θ range / °	3.98 – 72.0	2.02 – 28.33	3.64 – 75.81
T / K	100(2)	100(2)	293(2)
Diffractometer type	D8 Venture	D8 Venture	Xcalibur Nova
Range of *h*, *k*, *l*	−13 < *h* < 13; −17 < *k* < 17; −22 < *l* < 23	−34 < *h* < 35; −12 < *k* < 12; −52 < *l* < 52	−23 < *h* < 31; −9 < *k* < 9; −21 < *l* < 20
Reflections collected	39,263	204,889	14,595
Independent reflections	10,637	25,132	3155
Observed reflections ($I \geq 2\sigma$)	6063	17,512	3067
Absorption correction	none	none	Multi-scan
T_{min}, T_{max}	–	–	0.6899; 1.0000
R_{int}	0.0903	0.0550	0.0234
R (F)	0.0596	0.0380	0.0292
R_w (F^2)	0.2878	0.0910	0.0811
Goodness of fit	1.043	1.018	1.092
H atom treatment	Constrained	Mixed	Constrained
No. of parameters, restraints	806, 0	1531, 39	236, 1
Δρmax , Δρmin, Δρrms (e$Å^{-3}$)	1.060; −0.829; 0.090	0.651; − 0.794; 0.082	0.385; −0.571; 072
Compound	**4-RT**	**4-LT**	
Empirical formula	$C_{28}H_{44}Cl_4FeNO_{12}$	$C_{28}H_{44}Cl_4FeNO_{12}$	
Formula wt. / g mol^{-1}	784.29	784.29	
Colour	brown	brown	
Crystal dimensions / mm	0.20 × 0.18 × 0.08	0.21 × 0.12 × 0.07	
Space group	$P\bar{1}$	$P\bar{1}$	
a / Å	10.6942(7)	10.4469(11)	
b / Å	11.5080(7)	11.4073(12)	
c / Å	16.3692(11)	16.6390(17)	
α / °	76.833(6)	75.811(4)	
β / °	76.894(6)	80.356(4)	
γ / °	72.729(6)	67.620(4)	
Z	2	2	
V / $Å^3$	1845.5(2)	1771.5(3)	
D_{calc} / g cm^{-3}	1.411	1.470	
λ / Å	1.54179 (CuKα)	0.71073 (Mo*K*α)	
μ/ mm^{-1}	6.429	0.786	
Θ range / °	4.08 – 76.32	1.27 – 28.00	
T / K	293(2)	100(2)	
Diffractometer type	Xcalibur Nova	D8 Venture	
Range of *h*, *k*, *l*	−9 < *h* < 13; −13 < *k* < 14; −19 < *l* < 20	−15 < *h* < 13; −15 < *k* < 16; −23 < *l* < 24	
Reflections collected	18,554	18,665	
Independent reflections	7612	8359	
Observed reflections ($I \geq 2\sigma$)	6557	4383	
Absorption correction	Multi-scan	none	
T_{min}, T_{max}	0.4382; 1.0000	–	
R_{int}	0.0589	0.0833	
R (F)	0.0840	0.0977	
R_w (F^2)	0.289	0.2871	
Goodness of fit	1.067	1.056	
H atom treatment	Mixed	Constrained	
No. of parameters, restraints	442, 12	427, 0	
Δρmax , Δρmin, Δρrms (e$Å^{-3}$)	1.072; − 0.588; 0.129	1.257; −0.977; 0.153	

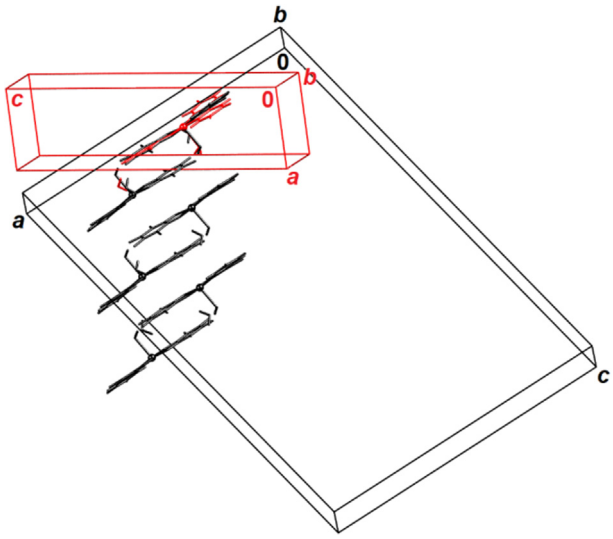

Fig. 1. Relation of the larger (correct, black) unit cell of compound **2** and the smaller (incorrect, red) one, arranged for maximum least-square overlap of the contents of smaller cell with molecule A of the large one. No is clear commensurate relation between two cells can be recognized.

compounds **1** and **2** were measured on a Bruker D8 Venture diffractometer (dual source; microfocus Mo tube used) equipped with and Oxford Cryosystems Series 700 liquid nitrogen cooling device. Program package SAINT [24] was used for data reduction and absorption correction. Two phases of compound **4** were identified: at low-temperature (100 K) **4-LT** and at room-temperature **4-RT**. Two different crystals were used to make data collection at these temperatures. Single crystal of **4-RT** was measured on the Oxford Diffraction Xcalibur Nova R diffractometer [23], while that of **4-LT** on the Bruker D8 Venture diffractometer [24].

The structures were solved using SHELXS97 [25] and refined with SHELXL-2017 [26]. Models were refined using the full-matrix least squares refinement; all non-hydrogen atoms were refined anisotropically. Hydrogen atoms bound to C atoms were modelled as riding entities using the AFIX command in SHELXL-2017 [26], while hydrogen atoms of water molecules were located in difference Fourier maps and refined with O—H bond length restrained to 0.92(2) Å and H—O—H angle restrained by restraining intramolecular H···H distance to 1.50(4) Å.

The unusual case of non-crystallographic symmetry and high Z' value for the structure of **2** indicate a possible erroneous choice of the unit cell, which was supported by the fact that approximately 1/6 of reflections were strong and other 5/6 much weaker (although not unobserved). Therefore, a refinement was attempted in a smaller unit cell [a = 7.2469(8) Å, b = 9.6501(13) Å, c = 24.173 (3) Å, β = 95.75(1)°], with 1/6 volume of the large cell [V = 1682.2 (5) Å^3; Table 1] and Z' = 1.

Both cells belong to the space group $P2_1/c$. However, transformation of one cell into the other is not straightforward; relation between them is shown in Fig. 1. Since refinement in the small cell yielded a poor structure with high R (9.1%) and very unrealistic displacement ellipsoids (Fig. S1), the larger cell was selected as correct.

Molecular geometry calculations were performed by PLATON [27,28] and molecular graphics were prepared using ORTEP-3 [29], and Mercury [30]. Analysis of Hirshfeld surfaces was carried out using the program package CrystalExplorer [31].

Crystallographic and refinement data for the structures reported in this paper are shown in Table 1.

CCDC 1988154–1988158 contains the supplementary crystallographic data for this paper. These data can be obtained free of charge via http://www.ccdc.cam.ac.uk/conts/retrieving.html (or from the CCDC, 12 Union Road, Cambridge CB2 1EZ, UK; Fax: +44 1223 336033; E-mail: deposit@ccdc.cam.ac.uk).

3. Results and discussion

3.1. Synthesis

By applying the layering technique, the dark red or brown crystals of acetonitrile-soluble compounds **1**–**4** were grown from the reaction of an acetonitrile solution of building block $[(n\text{-Bu})_4N]_3[M^{III}(C_6O_4Cl_2)_3]$ (M^{III} = Cr or Fe) and an aqueous solution containing $CuCl_2{\cdot}2H_2O$ and *N*-ligand [2,2′-bipyridine or 1,10-phenanthroline], in the molar ratio of 1:1:1. Unexpectedly, in a test tube partial decomposition of the used tris(chloranilato)metalate anions leads to the release of the chloranilate ligand from the metal coordination sphere. During the crystallization process, released chloranilate group from chromium(III) is consequently coordinated to copper(II) ion in the reaction mixture yielding $\{[Cu(bpy)(H_2O)(C_6O_4Cl_2)]{\cdot}H_2O\}_6$ (**2**), while that delivery from the coordination sphere of iron(III) causes the crystallization of chloranilate-based compound $[Cu(bpy)(C_6O_4Cl_2)]{\cdot}0{\cdot}5H_2O$ (**3**). This chloranilate release process is not usually observed for the tris(chloranilato)metalate precursor, but an analogous transfer occurs for tris(oxalato)chromate(III) and ferrate(III) used as building blocks during a diffusion in solution, under mild reaction conditions, such as slightly acidic pH and room temperature [17,18]. Crystals of compound $[(n\text{-Bu})_4N][Fe(H_2O)_2(C_6O_4Cl_2)_2]{\cdot}2H_2O$ (**4**) were utilized as a consequence of ligand exchange of the tris(chloranilato)ferrate(III) building block – chloranilate ligand coordinated to iron(III) was replaced by two water molecules. Black powder containing coordinated chloranilate and phenantroline ligand, as confirmed by IR spectroscopy, was also obtained as a result of this process.

Also, it appears that slow diffusion and the solvent mixture used herein causes formation of the crystals of the quality needed for X-ray analysis of the starting compound $[(n\text{-Bu})_4N]_3[Cr(C_6O_4Cl_2)_3]$ (**1**), whose crystal structure has not been known.

The IR spectra of the investigated complexes are in agreement with the results of the X-ray analysis and show the absorption bands that can be attributed to the vibrations of the bidentate chloranilate groups in **1**–**4** [22], and to those originating from coordinated 2,2′-bipyridine ligands in **2** and **3**. All absorption bands observed in the IR spectra of **1**–**4** are given in the Experimental section.

3.2. Molecular and crystal structure of compounds *1*–*4*

Asymmetric unit of the building block $[(n\text{-Bu})_4N]_3[Cr(C_6O_4Cl_2)_3]$ (**1**) comprises one $[Cr(C_6O_4Cl_2)_3]^{3-}$ complex anion and three $[(n\text{-Bu})_4N]^+$ cations (Figs. S2 and S3). The central chromium atom has a common distorted octahedral coordination (Table S1), and the complex anion has an approximate symmetry D_3 with three chloranilate moieties (designated as A, B and C) identical within experimental error. Since the structure lacks strong proton donors, it is dominated by C—H···O and C—H···Cl intermolecular interactions; there is also a weak type I halogen···halogen contacts between atoms Cl1B and Cl2A (symmetry operator: $-1 + x, y, z$) with distance of 3.376(3) Å. The complex anions are inserted into a "matrix" of cations (Fig. 1a). Analysis of Hirshfeld surface (HS; Fig. S8) shows that the bulk of intermolecular contacts to $[Cr(C_6O_4Cl_2)_3]^{3-}$ complex are C—H···O and C—H···Cl (comprising 39.0 and 38.1% of the HS, respectively; Fig. 2b and 2c). The chlorine···chlorine contact comprises 2.2% of the surface (Fig. 2d).

The compound $\{[Cu(bpy)(H_2O)(C_6O_4Cl_2)]{\cdot}H_2O\}_6$ (**2**) displays an interesting case of hypersymmetry with Z' = 6. Its asymmetric unit comprises 6 molecules of the complex $[Cu(bpy)(H_2O)(C_6O_4Cl_2)]$

(designated by letters A–F, Fig. S4 and Table S1) and 6 crystallization water molecules. They are related by five non-crystallographic (i.e. local) inversion centres with approximate coordinates (0.80, 0.45, 0.08), (0.82, 0.45, 0.17), (0.87, 0.45, 0.25), (0.92, 0.45, 0.33) and (0.96, 0.45, 0.96).

The copper(II) atoms have a square-pyramidal coordination with the water molecule occupying the apical position. This compound was previously reported as methanol solvate with $Z' = 1$ [19]. However, due to the presence of dissimilar solvent molecules, crystal packing differs significantly. Crystal packing of **2** is dominated by hydrogen-bonded chains extending in the direction [0 1 0]. There are three symmetry-independent chains (related by non-crystallographic symmetry), each formed by a pair of molecules related by a local inversion: AB, CD and EF, and two uncoordinated water molecules (Fig. 3a, Table 2). These chains involve pairs of complex molecules related by a local inversion (e.g. A and B) linked by two hydrogen bonds with coordinated water molecules acting as donors and carbonyl oxygens acting as acceptors; the pairs are linked to each other by uncoordinated water molecules which act both as hydrogen bond donors and acceptors (Fig. 3b, Table 2). The chains stack through interactions between chloranilate and bpy moieties (Fig. 3a, Table 3), forming layers parallel to $(20\bar{3})$. A 3D packing is completed by weaker stacking interactions involving bpy moieties of different layers (Table 3).

Asymmetric unit of **3** contains one neutral molecule of [Cu(bpy)($C_6O_4Cl_2$)] and a half of a crystallization water molecule (located on a twofold axis, Fig. S5). Molecular geometry of the square-planar coordination sphere of copper(II) complex (Table S1) is in a good agreement with the previously studied anhydrous complex [Cu(bpy)($C_6O_4Cl_2$)] [19], however crystal packing is different due to the presence of a water molecule which acts as a double proton donor of two bifurcated hydrogen bonds towards two neighbouring [Cu(bpy)($C_6O_4Cl_2$)] molecules. Thus are formed discrete dimeric motives (Fig. 4a). The molecules form infinite π-stacks in the direction [010] with short contacts bpy···chloranilate, chloranilate···chelating ring, and chelating ring... chelating ring (Fig. 4b,

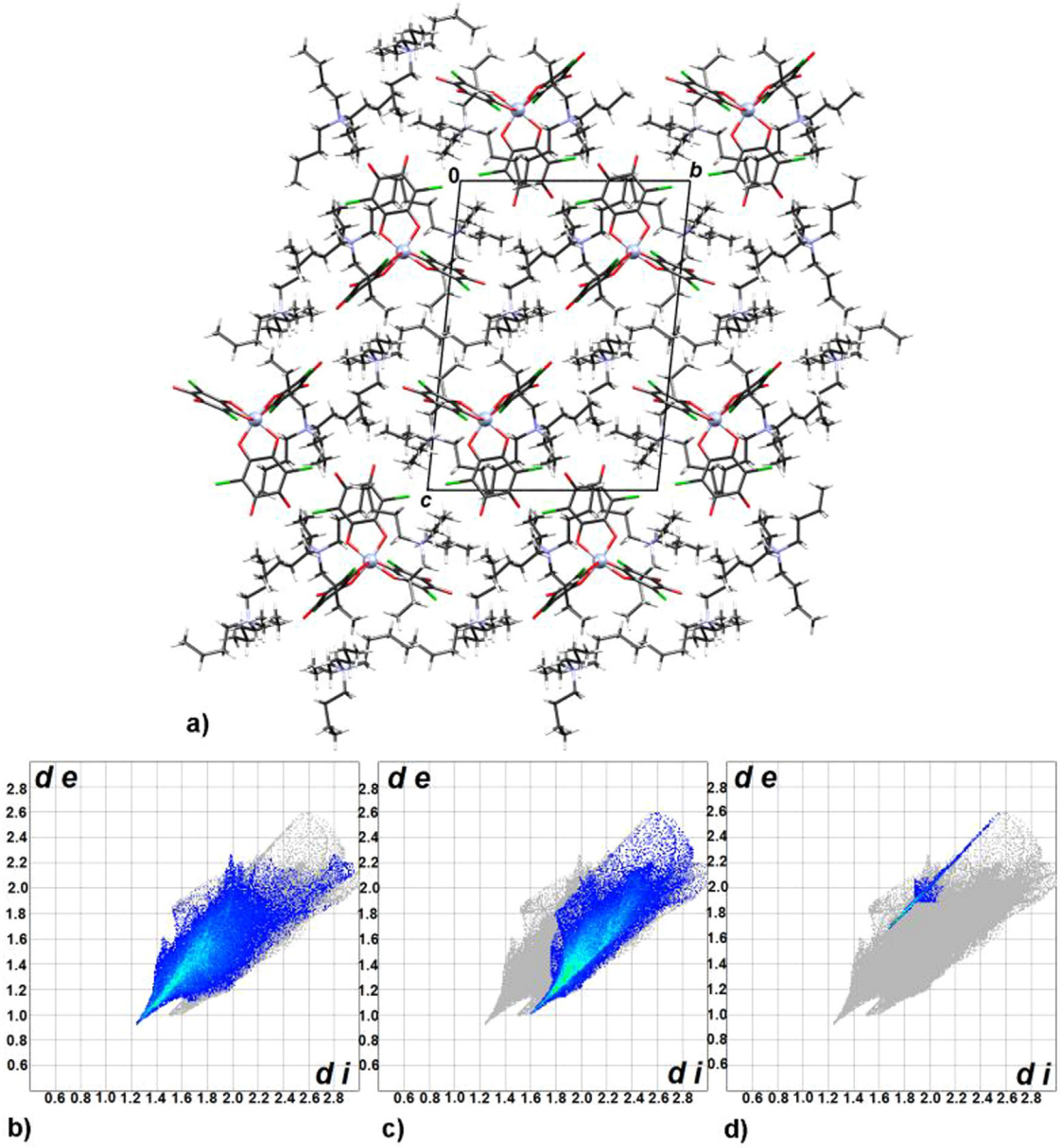

Fig. 2. a) Crystal packing of compound **1** viewed in the direction [100]. Fingerprint plots of intermolecular interactions: b) H···O, c) H···Cl and d) Cl···Cl.

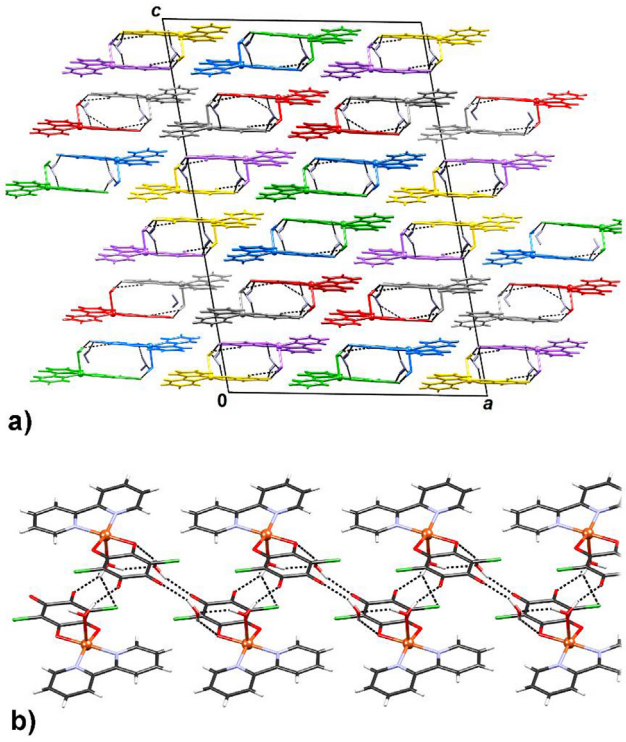

Fig. 3. Crystal packing of compound **2** a) viewed in the direction [0 1 0] (i.e. along the hydrogen-bonded chains) and b) a close-up view of a chain comprising of molecules A (above) and B (below). Molecules in a) are colour-coded for clarity: A are green, B are blue, C are red, D are gray, F are purple and F are yellow. Uncoordinated water molecules are shown as blue-gray and hydrogen bonds are shown as black dotted lines.

Table 3). These contacts and their geometry are similar to those observed in the anhydrous compound [19]; analysis of Hirshfeld surfaces and Voronoi-Dirichlet polyhedra showed that these stacking interactions are of dominantly electrostatic nature and considerably stronger than stacking of aromatic rings [7,8]. Hirshfeld surface of [Cu(bpy)($C_6O_4Cl_2$)] molecule in **3** (Fig. S9) involves an unusually high contribution of C···C contacts of 7.3%, and relatively less H···O and H···Cl contacts (21.7 and 17.5%, respectively), illustrating importance of stacking interactions in crystal packing (Fig. 4c).

Compound **4** comprises a complex anion $[Fe(H_2O)_2(C_6O_4Cl_2)_2]^-$ and a $(n\text{-}Bu)_4N^+$ cation (Figs. S5 and S6); it crystallizes as a dihydrate. Chloranilate moieties in the anion are arranged in *cis*-position, and two coordinated water molecules are also in a *cis*-position, so the centrosymmetric crystals are in fact racemic. A number of compounds comprising the $[Fe(H_2O)_2(C_6O_4Cl_2)_2]^-$ anion have been studied previously. Tetrahydrates of its Rb and Cs salts [32] and also organic–inorganic hybrid compounds with tetrathiafulvalene, ferrocene, decamethylferrocene [33] and phenazine [33,34] have a *trans*-arrangement of chloranilate groups. *Cis*-arrangement of these moieties has been found in the salts $Rb_2[Fe(H_2O)_2(C_6O_4Cl_2)_2]_2{\cdot}5H_2O$ [32] and $(H_2bpy)[Fe(H_2O)_2(C_6O_4Cl_2)_2]_2{\cdot}2H_2O$ (bpy = 4,4′-bipyridine) [35]. In these two compounds molecular geometry of the $[Fe(H_2O)_2(C_6O_4Cl_2)_2]^-$ anions are very similar.

Two phases of compound **4** were identified: at low-temperature (100 K) **4-LT** and at room-temperature **4-RT**. Unit-cell parameters are similar, but it can be noted that the axis *c* of the low-temperature phase is longer than in the RT phase (Table 1). However, different positions and orientations of water molecules result in completely different hydrogen-bonding patterns: in **4-RT** complex anions and water molecules form chains extending in direction [0$\bar{1}$2] (Fig. 5a, Table 2), while in **4-LT** there are hydrogen-bonded layers parallel to (100) (Fig. 5b, Table 2). In both structures there are seven symmetry-independent hydrogen bonds (Table 2). Both crystal packings are layered with alternating hydrophilic (complex anions and water molecules) and hydrophobic (cations) layers parallel to (100). However, in **4-LT** there is an additional π-stacking contact (Table 3) between two chloranilate groups, which is not found in **4-RT** (i.e. the shortest centroid–centroid distance is about 4.5 Å). Differences in intermolecular interactions in two phases can be noted in different Hirshfeld surfaces of the $[Fe(H_2O)_2(C_6O_4Cl_2)_2]^-$ anions (Figures S10 and S11). Hydrogen bonding is the dominant interaction, so the contacts H···O form the largest part of the HS; however they are more prevalent in **4-RT** than **4-LT** (covering 37.7 and 32.6% of the HS, respectively). Situation with C···C contacts (corresponding to π-stacking) is the opposite: their respective coverages of the HS are 1.9 and 3.3%. These differences are easily visualized by fingerprint plots (Fig. 6).

Table 2
Geometric parameters of hydrogen bonds (Å, °) for compounds **2**, **3** and **4**.

	D–H / Å	H···*A* / Å	*D*···*A* / Å	*D*–H···*A* / °	Symm. op. on *A*
2					
O7A–H7A2···O8	0.93(2)	1.92(2)	2.801(3)	158(3)	*x*, −1 + *y*, *z*
O7A–H7A1···O3B	0.86(3)	1.91(2)	2.718(3)	157(2)	*x*, *y*, *z*
O7B–H7B2···O9	0.91(2)	1.95(2)	2.802(3)	156(3)	*x*, 1 + *y*, *z*
O7B–H7B1···O3A	0.92(3)	1.82(3)	2.720(3)	165(3)	*x*, *y*, *z*
O7C–H7C2···O10	0.93(2)	1.90(2)	2.793(3)	160(3)	*x*, *y*, *z*
O7C–H7C1···O3D	0.87(3)	1.90(2)	2.696(3)	152(2)	*x*, *y*, *z*
O7D–H7D2···O11	0.93(2)	1.92(2)	2.794(3)	157(3)	*x*, 1 + *y*, *z*
O7D–H7D1···O3C	0.91(3)	1.86(3)	2.729(3)	161(3)	*x*, *y*, *z*
O7E–H7E2···O12	0.92(2)	1.91(2)	2.784(3)	158(3)	*x*, *y*, *z*
O7E–H7E1···O3F	0.86(3)	1.89(2)	2.705(3)	157(2)	*x*, *y*, *z*
O7F–H7F2···O13	0.91(2)	1.94(2)	2.790(3)	155(3)	*x*, *y*, *z*
O7F–H7F1···O3E	0.92(2)	1.82(2)	2.703(3)	160(2)	*x*, *y*, *z*
O8–H8A2···O4B	0.90(3)	1.92(3)	2.784(3)	161(3)	*x*, *y*, *z*
O8–H8A1···O1A	0.91(3)	2.02(3)	2.833(3)	147(3)	*x*, 1 + *y*, *z*
O9–H9A1···O4A	0.90(3)	1.94(3)	2.787(3)	155(3)	*x*, *y*, *z*
O9–H9A2···O1B	0.92(3)	2.05(3)	2.835(3)	143(3)	*x*, −1 + *y*, *z*
O10–H101···O4D	0.90(3)	1.93(3)	2.797(3)	160(3)	*x*, −1 + *y*, *z*
O10–H102···O1C	0.93(3)	2.06(3)	2.862(3)	144(3)	*x*, *y*, *z*
O11–H111···O1D	0.93(3)	2.08(3)	2.876(3)	143(3)	*x*, −1 + *y*, *z*
O11–H112···O4C	0.92(3)	1.91(3)	2.787(3)	159(3)	*x*, *y*, *z*
O12–H121···O1E	0.92(3)	2.17(3)	2.903(3)	136(3)	*x*, *y*, *z*
O12–H122···O4F	0.93(3)	1.93(3)	2.811(3)	157(3)	*x*, −1 + *y*, *z*
O13–H131···O4E	0.91(3)	1.94(3)	2.808(3)	157(3)	*x*, 1 + *y*, *z z*
O13–H131···O1F	0.92(3)	2.15(3)	2.906(3)	139(3)	*x*, *y*, *z*
4-LT					
O5–H5A···O4A	0.85	1.87	2.662(7)	155	1 − *x*,1 − *y*, −*z*
O6–H6B···O8	0.85	1.84	2.669(8)	163	*x*, *y*, *z*
O7–H7A···O8	0.85	2.13	2.904 (12)	151	*x*, *y*, *z*
O7–H7B···O4B	0.85	2.20	2.910 (11)	141	1 − *x*, −*y*,1 − *z*
O8–H8A···O3A	0.85	1.97	2.774 (11)	156	*x*, −1 + *y*, *z*
O8–H8B···O3A	0.85	2.34	3.044(9)	140	1 − *x*, 1 − *y*, −*z*
O8–H8B···O4A	0.85	2.14	2.843 (10)	140	1 − *x*, 1 − *y*, −*z*
4-RT					
O5–H5A···O3A	0.95(3)	1.77(4)	2.690(6)	160(6)	1 − *x*, −*y*,1 − *z*
O5–H5B···O7	0.95(4)	1.71(4)	2.620(7)	159(7)	*x*, *y*, *z*
O6–H6B···O3B	0.94(7)	1.76(7)	2.681(7)	169(10)	1 − *x*, 1 − *y*, −*z*
O7–H7D···O3B	0.95(7)	2.54 (10)	3.139(8)	121(8)	1 − *x*, 1 − *y*, −*z*
O7–H7D···O4B	0.95(7)	1.95(7)	2.882(8)	167(9)	1 − *x*,1 − *y*, −*z*
O8–H8C···O3A	0.95(6)	2.28 (11)	2.908(9)	123(8)	1 − *x*, −1 − *y*, −*z*
O8–H8C···O4A	0.95(6)	2.21(6)	3.004(7)	140(9)	1 − *x*, −1 − *y*, −*z*

Table 3
Geometric parameters of π-stacking (Å, °).

π···π	Cg[a]···Cg / Å	α[b]	β[c]	Cg···plane(Cg2) / Å	Offset/ Å[d]	Symm. op. on Cg2
2						
N1A → C11A···N2E → C11E	3.8242(15)	23.29(12)	16.7	3.2467(10)	–	1 − *x*, −1/2 + *y*, 1/2 − *z*
N2A → C16A···N1E → C16E	3.8369(15)	23.55(12)	28.9	3.6318(10)	–	1 − *x*, 1/2 + *y*, 1/2 − *z*
N1B → C11B···N1F → C11F	3.8014(15)	23.32(12)	15.3	3.2593(11)	–	2 − *x*, −1/2 + *y*, 1/2 − *z*
N2B → C16B···C2F → C16F	3.8074(15)	23.18(12)	28.3	3.6268(10)	–	2 − *x*, −1/2 + *y*, 1/2 − *z*
N1C → C11C···N2C → C16C	3.8327(16)	22.68(13)	18.0	3.2967(11)	–	1 − *x*, −1/2 + *y*, 1/2 − *z*
Cu4 → O2D···Cu5 → O2E	3.8193(13)	0.79(10)	31.5	3.2301(9)	1.996	*x*, *y*, *z*
Cu4 → N2D···C1E → C6E	3.8772(15)	8.59(11)	28.0	3.1159(9)	1.819	*x*, *y*, *z*
N1D → C11D···N2D → C16D	3.8008(16)	23.69(13)	16.3	3.3120(11)	–	2 − *x*, 1/2 + *y*, 1/2 − *z*
N2D → C16D···C1E → C6E	3.9665(15)	4.72(12)	34.0	3.3066(11)	2.217	*x*, *y*, *z*
C1D → C6D···Cu5 → N2E	3.9230(15)	7.89(11)	37.5	3.4078(10)	2.387	*x*, *y*, *z*
C1D → C6D···N2E → C11E	4.0182(15)	4.86(12)	34.7	3.2599(10)	2.287	*x*, *y*, *z*
Cu5 → N2E···Cu4 → O2D	3.8195(13)	0.79(10)	32.3	3.2565(9)	2.038	*x*, *y*, *z*
Cu5 → O5E···C1D → C6D	4.1693(15)	1.55(11)	38.5	3.2041(9)	2.596	*x*, *y*, *z*
Cu5 → N2E···C1D → C6D	3.9229(15)	7.89(11)	29.7	3.1129(9)	1.943	*x*, *y*, *z*
Cu6 → O2F···Cu6 → O2F	3.7487(13)	0	31.1	3.2088(9)	1.938	2 − *x*, 1 − *y*, 1 − *z*
Cu6 → O2F···C1F → C6F	4.1324(14)	2.92(10)	37.6	3.1543(9)	2.522	2 − *x*, 1 − *y*, 1 − *z*
Cu6 → N2F···C1F → C6F	3.8501(14)	7.78(11)	28.4	3.1144(9)	1.832	2 − *x*, 1 − *y*, 1 − *z*
N1F → C11F···C1F → C6F	3.9786(15)	4.80(12)	35.1	3.3119(10)	2.290	2 − *x*, 1 − *y*, 1 − *z*
3						
Cu1 → O2···Cu1 → O2	3.4057(8)	0.03(7)	20.6	3.1876(6)	1.199	−*x*, 2 − *y*, −*z*
Cu1 → O2···N2 → C16	3.8754(9)	1.43(7)	35.0	3.1703(6)	2.224	−*x*, 2 − *y*, −*z*
Cu1 → N2···C1 → C6	3.5588(9)	1.60(7)	27.4	3.1191(6)	1.637	−*x*, 2 − *y*, −*z*
N2 → C16···C1 → C6	3.3951(10)	2.81(8)	9.0	3.3727(8)	0.530	−*x*, 1 − *y*, −*z*
4-LT						
C1B → C6B···C1B → C6B	3.535(5)	0	22.0	3.278(4)	1.233	1 − *x*, −*y*, 1 − *z*

[a] Cg = centre of gravity of the aromatic ring.
[b] α = angle between planes of two interacting rings.
[c] β = angle between Cg···Cg line and normal to the plane of the first interacting ring.
[d] Offset can be calculated only for the strictly parallel rings (α = 0.00°). For slightly inclined rings (α ≤ 5°) an approximate value is given.

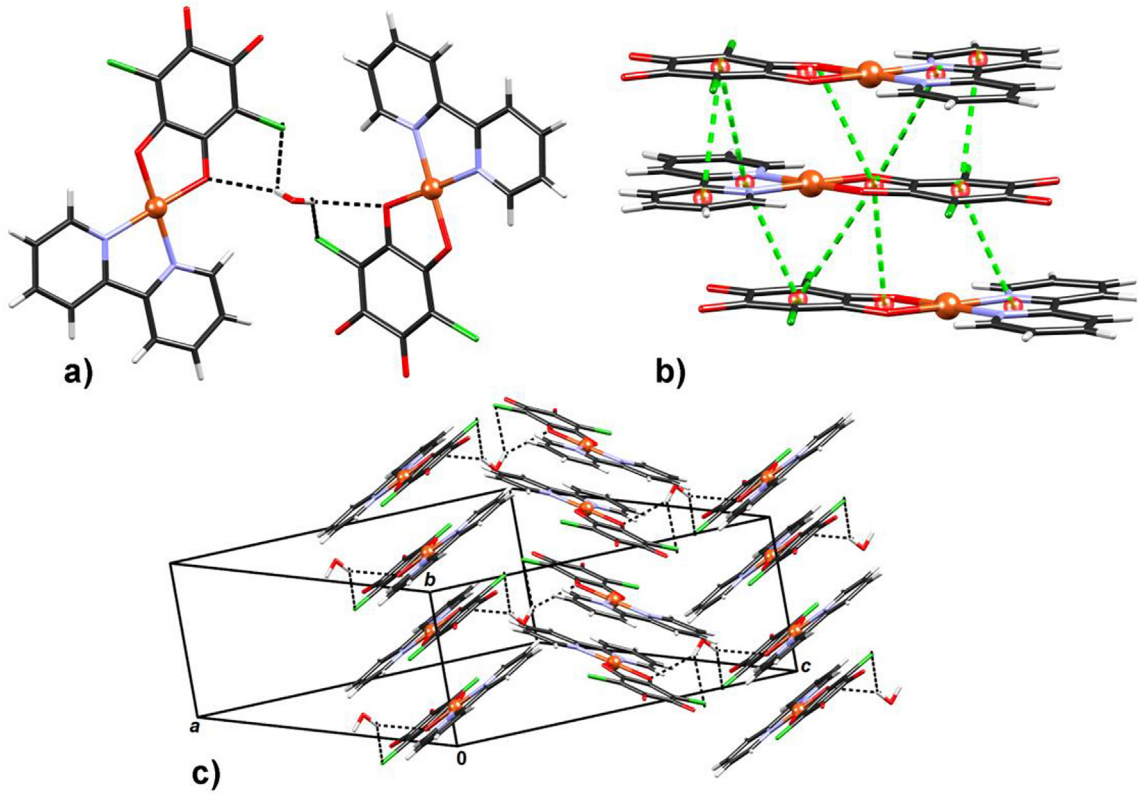

Fig. 4. Crystal packing of compound **3**: a) hydrogen bonded dimer bridged by a water molecule, b) a detail of π-stacking showing close contacts between different types of rings and c) overall packing motive formed by stacking of hydrogen bonded dimers. Specific stacking contacts are shown as green dashed lines connecting ring centroids (shown as red spheres).

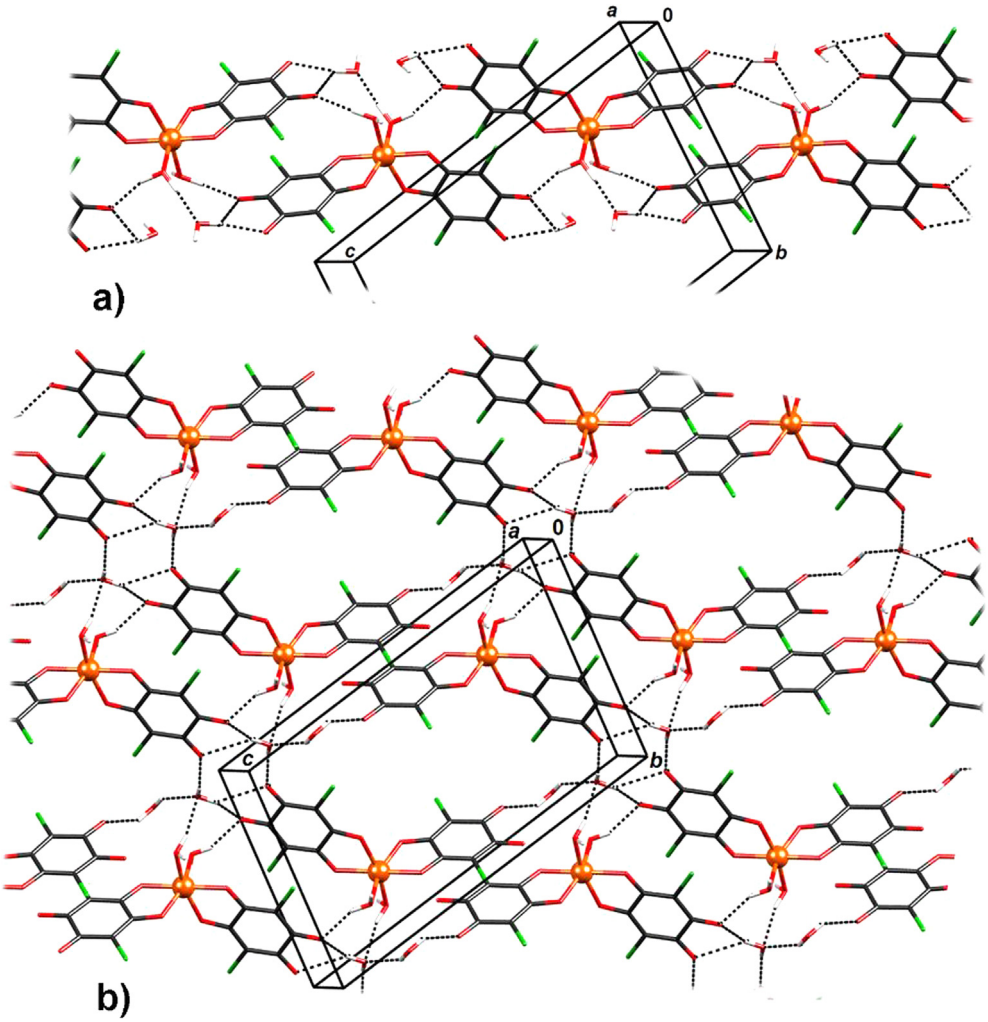

Fig. 5. Hydrogen bonding patterns in compound **4**: a) 1D motive in high-temperature phase (**4-RT**) and b) 2D motive in low-temperature phase (**4-LT**).

4. Conclusions

We have prepared and characterized three novel chloranilate-based mononuclear complexes with copper(II) and iron(III) cations, but five novel crystal structures, including the previously known compound **1** and two phases of the same compound **4**, have been described. Study of crystal packing points out to importance of π-stacking interactions involving the chloranilate moiety, which play an important role alongside the common hydrogen bonding. Analysis of Hirshfeld surfaces facilitated and supplemented analysis of crystal structures, and enabled visualisation of most common types of intermolecular contacts. Thus, the dominant contacts in **1** and two phases of **4** are H···O, corresponding to hydrogen bonding; however, in **3** there is a considerable proportion of C···C contacts, corresponding to π-stacking interactions. In addition, the compound **2** is an interesting case-study of hypersymmetry, with Z' = 6 and as many as five non-crystallographic (local) inversion centres in the asymmetric unit.

Our further research will be related to the synthesis and characterization of novel homo- and heterometallic compounds obtained using building blocks $[M^{III}(C_6O_4Cl_2)_3]^{3-}$ (M^{III} = Cr and Fe), that are expected to have especially interesting structural and magnetic properties, since these systems are still insufficiently explored.

CRediT authorship contribution statement

Lidija Kanižaj: Conceptualization, Investigation. **Vedran Vuković:** Investigation, Formal analysis. **Emmanuel Wenger:** Investigation, Formal analysis. **Marijana Jurić:** Conceptualization, Supervision, Writing - original draft. **Krešimir Molčanov:** Writing - original draft, Visualization, Funding acquisition.

Declaration of Competing Interest

The authors declare that they have no known competing financial interests or personal relationships that could have appeared to influence the work reported in this paper.

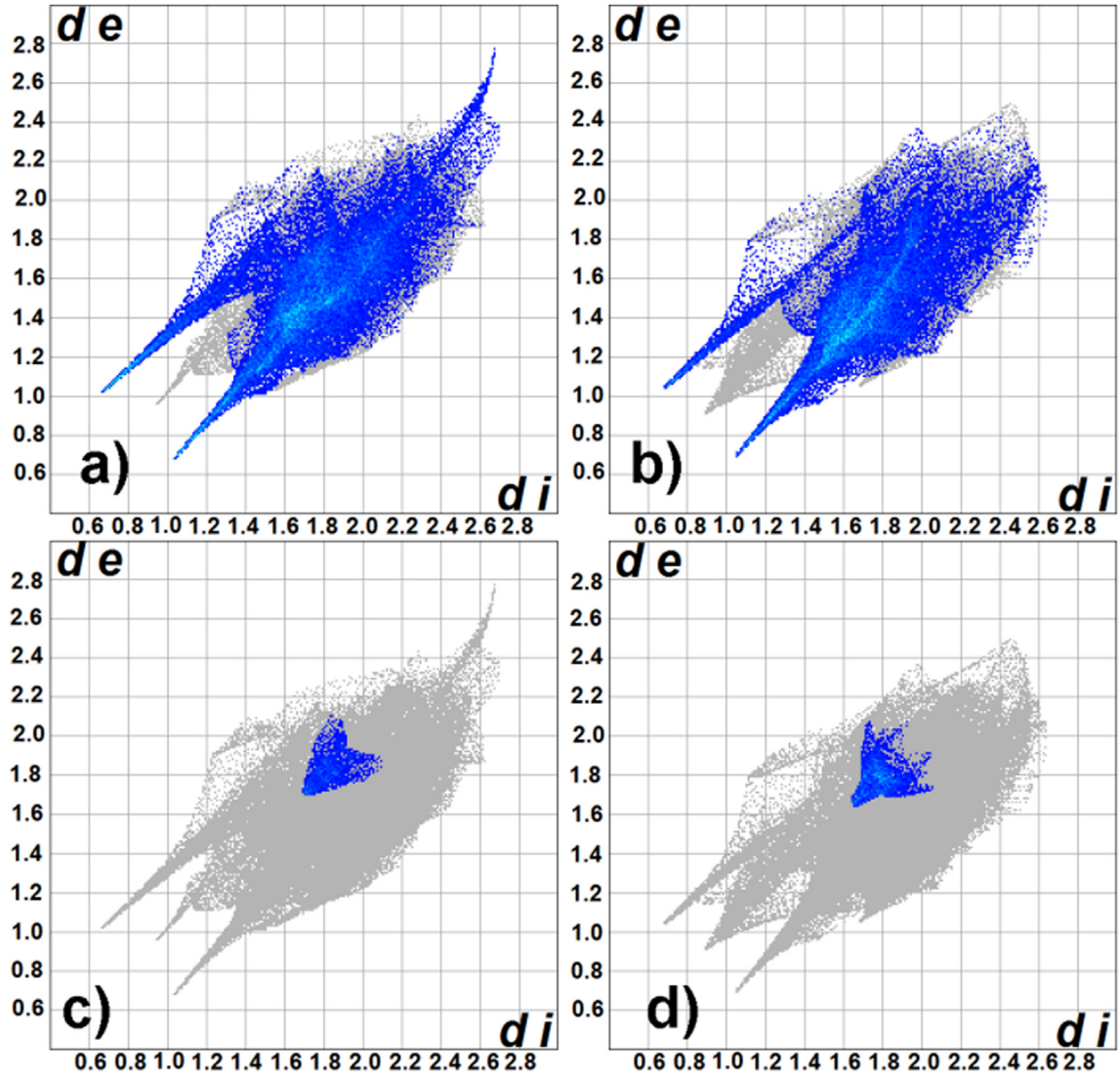

Fig. 6. Fingerprint plots of intermolecular contacts in **4-RT** (a and c) and **4-LT** (b and d). Top row represent contacts H···O and lower row represents contacts C···C.

Acknowledgements

This research was funded by the Croatian Science Foundation under project No. IP-2014-09-4079. L.K. acknowledges L'Oréal ADRIA d.o.o. and Croatian Commission for UNESCO for a scholarship.

Appendix A. Supplementary data

Supplementary data to this article can be found online at https://doi.org/10.1016/j.poly.2020.114723.

References

[1] E. Coronado, G.M. Espallargas, Dynamic magnetic MOFs, Chem. Soc. Rev. 42 (2013) 1525–1539.
[2] G.M. Espallargas, E. Coronado, Magnetic functionalities in MOFs: from the framework to the pore, Chem. Soc. Rev. 47 (2018) 533–557.
[3] C.R. Groom, I.J. Bruno, M.P. Lightfoot, S.C. Ward, The Cambridge Structural Database, Acta Crystallogr., Sect. B: Struct. Sci., Cryst. Eng. Mater. 72 (2016) 171–179.
[4] M. Clemente-León, E. Coronado, C. Martí-Gastaldoz, F.M. Romero, Multifunctionality in hybrid magnetic materials based on bimetallic oxalate complexes, Chem. Soc. Rev. 40 (40) (2011) 473–497.
[5] V. Vuković, K. Molčanov, C. Jelsch, E. Wenger, A. Krawczuk, M. Jurić, L. Androš Dubraja, B. Kojić-Prodić, Malleable Electronic Structure of Chloranilic Acid and Its Species Determined by X-ray Charge Density, Cryst. Growth Des. 19 (2019) 2802–2810.
[6] M.L. Mercuri, F. Congiu, G. Concas, S.A. Sahadevan, Recent Advances on Anilato-Based Molecular Materials with Magnetic and/or Conducting Properties, Magnetochemistry 3 (2017) 17.
[7] K. Molčanov, V. Milašinović, B. Kojić-Prodić, Contribution of Different Crystal Packing Forces in π-Stacking: From Noncovalent to Covalent Multicentric Bonding, Cryst. Growth Des. 19 (2019) 5967–5980.
[8] K. Molčanov, B. Kojić-Prodić, Towards understanding π-stacking interactions between non-aromatic rings, IUCrJ 6 (2019) 156–166.
[9] S. Benmansour, C. Vallés-García, P. Gómez-Claramunt, G. Mínguez Espallargas, C.J. Gómez-García, 2D and 3D Anilato-Based Heterometallic M(I)M(III) Lattices: The Missing Link, Inorg. Chem. 54 (2015) 5410–5418.
[10] A. Abhervé, M. Clemente-León, E. Coronado, C.J. Gómez-García, M. Verneret, One-Dimensional and Two-Dimensional Anilate-Based Magnets with Inserted Spin-Crossover Complexes, Inorg. Chem. 53 (2014) 12014–12026.
[11] M. Atzori, S. Benmansour, G. Mínguez Espallargas, M. Clemente-León, A. Abhervé, P. Gómez-Claramunt, E. Coronado, F. Artizzu, E. Sessini, P. Deplano, A. Serpe, M.L. Mercuri, C.J. Gómez García, A Family of Layered Chiral Porous Magnets Exhibiting Tunable Ordering Temperatures, Inorg. Chem. 52 (2013) 10031–10040.
[12] K. Molčanov, M. Jurić, B. Kojić-Prodić, A novel type of coordination mode of chloranilic acid leading to the formation of polymericcoordination ribbon in the series of mixed-ligand copper(II) complexes with 1,10-phenanthroline, Dalton Trans. 43 (2014) 7208–7218.
[13] (a) S. Kitagawa, S. Kawata, Coordination compounds of 1,4-dihydroxybenzoquinone and its homologues, Structures and properties. Coord. Chem. Rev. 224 (2002) 11–34;

(b) B.F. Abrahams, T.A. Hudson, L.J. McCormick, R. Robson, Coordination Polymers of 2,5-Dihydroxybenzoquinone and Chloranilic Acid with the (10,3)-a Topology, Cryst. Growth Des. 11 (2011) 2717–2720;
(c) C.J. Kingsbury, B.F. Abrahams, D.M. D'Alessandro, T.A. Hudson, R. Murase, R. Robson, K.F. White, Role of NEt4+ in Orienting and Locking Together [M2lig3]2– (6,3) Sheets (H2lig = Chloranilic or Fluoranilic Acid) to Generate Spacious Channels Perpendicular to the Sheets Cryst, Growth Des. 17 (2017) 1465–1470.

[14] A. Podborska, M. Suchecki, K. Mech, M. Marzec, K. Pilarczyk, K. Szaciłowski, Light intensity-induced photocurrent switching effect, Nature Commun. 11 (2020) 854.

[15] J. Habjanič, M. Jurić, J. Popović, K. Molčanov, D. Pajić, A 3D Oxalate-Based Network as a Precursor for the $CoMn_2O_4$ Spinel: Synthesis and Structural and Magnetic Studies, Inorg. Chem. 53 (2014) 9633–9643.

[16] M. Jurić, D. Pajić, D. Žilić, B. Rakvin, K. Molčanov, J. Popović, Magnetic order in a novel 3D oxalate-based coordination polymer$\{[Cu(bpy)_3][Mn_2(C_2O_4)_3]\cdot H_2O\}_n$, Dalton Trans. 44 (2015) 20626–20635.

[17] L. Kanižaj, K. Molčanov, F. Torić, D. Pajić, I. Lončarić, A. Šantića, M. Jurić, Ladder-like [CrCu] coordination polymerscontaining unique bridging modes of $[Cr(C_2O_4)_3]^{3-}$ and $Cr_2O_7^{2-}$, Dalton Trans. 48 (2019) 7891–7898.

[18] L. Kanižaj, L. Androš Dubraja, F. Torić, D. Pajić, K. Molčanov, E. Wenger, M. Jurić, Dimensionality controlled by light exposure: 1Dversus 3D oxalate-bridged [CuFe] coordination polymers based on an $[Fe(C_2O_4)_3]^{3-}$ metallotecton, Inorg. Chem. Front. 6 (2019) 3327–3335.

[19] K. Molčanov, M. Jurić, B. Kojić-Prodić, Stacking of metal chelating rings with π-systems in mononuclear complexes of Cu(II) with 3,6-dichloro-2,5-dihydroxy-1,4-benzoquinone (chloranilic acid) and 2,2'-bipyridine ligands, Dalton Trans. 42 (2013) 15756–15765.

[20] L. Androš Dubraja, K. Molčanov, D. Žilić, B. Kojić-Prodić, E. Wenger, Multifunctionality and size of the chloranilate ligand define the topology of transition metal coordination polymers, New J. Chem. 41 (2017) 6785–6794.

[21] M. Jurić, K. Molčanov, D. Žilić, B. Kojić-Prodić, From mononuclear to linear one-dimensional coordination species of copper(II)-chloranilate: design and characterization, RSC Adv. 6 (2016) 62785–62796.

[22] M. Atzori, F. Artizzu, E. Sessini, L. Marchiò, D. Loche, A. Serpe, P. Deplano, G. Concas, F. Pop, N. Avarvari, M.L. Mercuri, Halogen-bonding in a new family of tris(haloanilato)metallate(iii) magnetic molecular building blocks, Dalton Trans. 43 (2014) 7006–7019.

[23] O.D. Rigaku, P.R.O. CrysAlis, Rigaku Oxford Diffraction Ltd, Yarnton, England, 2018.

[24] Bruker, SAINT V8.34A, Bruker AXS Inc., Madison, WI, 2013.

[25] G. M. Sheldrick, SHELXT - Integrated space-group and crystal structure determination. Acta Crystallogr., Sect. A: Found. Adv. 71 (2015) 3–8.

[26] G.M. Sheldrick, Crystal structure refinement with *SHELXL*, Acta Crystallogr., Sect. C 71 (2015) 3–8.

[27] A.L. Spek, Single-crystal structure validation with the program *PLATON*, J. Appl. Crystallogr. 36 (2003) 7–13.

[28] A.L. Spek, Structure validation in chemical crystallography, Acta Crystallogr. Sect. D 65 (2009) 148–155.

[29] L.J. Farrugia, ORTEP3 for Windows - a version of ORTEP III with a Graphical User Interface (GUI), J. Appl. Crystallogr. 30 (1997) 565.

[30] C.F. Macrae, I. Sovago, S.J. Cottrell, P.T.A. Galek, P. McCabe, E. Pidcock, M. Platings, G.P. Shields, J.S. Stevens, M. Towler, P.A. Wood, *Mercury 4.0*: from visualization to analysis, design and prediction, J. Appl. Crystallogr. 53 (2020) 226–235.

[31] M.A. Spackman, J.J. McKinnon, D. Jayatilaka, Electrostatic potentials mapped on Hirshfeld surfaces provide direct insight into intermolecular interactions in crystals, CrystEngComm 10 (2008) 377–388.

[32] Z.K. Nikitina, G.V. Shilov, N.S. Ovanesyan, V.D. Makhaev, Synthesis and some properties of anionic chloranilate complexes of iron(iii). Crystal and molecular structure of rubidium and cesium chloranilatoferrates, Russ. Chem. Bull. 62 (2013) 419–426.

[33] K. Nagayoshi, Md.K. Kabir, H. Tobita, K. Honda, M. Kawahara, M. Katada, K. Adachi, H. Nishikawa, I. Ikemoto, H. Kumagai, Y. Hosokoshi, K. Inoue, S. Kitagawa, S. Kawata, Design of Novel Inorganic−Organic Hybrid Materials Based on Iron-Chloranilate Mononuclear Complexes: Characteristics of Hydrogen-Bond-Supported Layers toward the Intercalation of Guests, J. Am. Chem. Soc. 125 (2003) 221–232.

[34] M.K. Kabir, S. Kawata, K. Adachi, H. Tobita, N. Miyazaki, H. Kumagai, M. Katada, S. Kitagawa, Iron-Chloranilate Intercalation Compounds: Synthesis, Crystal Structures, and Thermal Properties, Mol. Cryst. Liq. Cryst. 341 (2000) 491–496.

[35] M.K. Kabir, N. Miyazaki, S. Kawata, K. Adachi, H. Kumagai, K. Inoue, S. Kitagawa, K. Iijima, M. Katada, Novel layered structures constructed from iron–chloranilate compounds, Coord. Chem. Rev. 198 (2000) 157–169.